

# Chapter 15

## Identification of Non-stationary and Non-linear Drying Processes



Piotr Wolszczak and Waldemar Samociuk

**Abstract** This chapter discusses a problem of control of a non-stationary and a non-linear drying process of food raw materials, especially yeast. Industrial yeast drying is a non-stationary and a non-linear process with a transport delay. In this work the identification of the yeast drying process was presented. Models for different time intervals of the closed control system were developed. Changes in the model parameters (non-stationarity) caused deterioration in the stability reserve. The developed models will be used to synthesize the control system in the future.

### 15.1 Introduction

The non-stationary and non-linear processes control is troublesome, especially if there is a transport delay and the process concerns a vivid material. Industrial drying of yeast is such a process. Active dried yeast (ADY) is used in industrial processes; in the craft brewing sector, distilling and baking industries and in wine production [12]. There is supply of warm air to the object during drying, too high temperature has an disadvantageous influence on its fermentation capacity [13]. Dried yeast vitality is influenced not only by the temperature value but also by the rate of its change [9, 19]. During industrial production, various types (strains) of yeast are used which are resistant to temperature to varying degrees [5, 24]. “Skim milk—a widely used protective agent—was used and in all strains, the highest viabilities following air-blast drying were obtained using 10% skim milk” [15]. Drying is continued until the dry weight of the yeast culture is approximately 93–95% dry weight [3] or 92–96% [2].

---

P. Wolszczak (✉)

Faculty of Mechanical Engineering, Lublin University of Technology, Nadbystrzycka 36, 20-618 Lublin, Poland  
e-mail: [p.wolszczak@pollub.pl](mailto:p.wolszczak@pollub.pl)

W. Samociuk

Faculty of Production Engineering, University of Life Sciences in Lublin, 28 Głęboka Street, 20-612 Lublin, Poland  
e-mail: [waldemar.samociuk@up.lublin.pl](mailto:waldemar.samociuk@up.lublin.pl)

© Springer Nature Singapore Pte Ltd. 2019

M. Belhaq (ed.), *Topics in Nonlinear Mechanics and Physics*,

Springer Proceedings in Physics 228, [https://doi.org/10.1007/978-981-13-9463-8\\_15](https://doi.org/10.1007/978-981-13-9463-8_15)

When designing control systems, a compromise between the complexity of the controlled process model and the effort necessary to obtain a reliable mathematical description is inevitable. Finding models from the laws of physics can be troublesome. For this reason, control systems based on the experimental data are designed. The indirect approach uses the collected data to identify the controlled process model, which is then used to synthesize the controller in accordance with the project objectives [1]. This method is based on the system identification tools ([4, 10, 11, 16–18, 25, 27]).

The selection of fixed parameters of the classic control system (PID) for the entire drying cycle can be impossible, therefore it is necessary to use complex control systems (Robust control, Adaptive Control, IMC) [25]. In addition, due to the process safety and high sensitivity of the material to a high temperature (over-regulation), it is advisable to use security systems (locks) at the appropriate SIL level [22, 23].

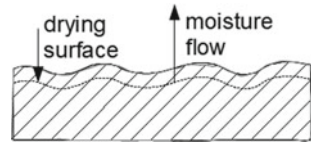
To enable high quality control it is necessary to know the object properties, saved in the form of an operator transfer function and the range of changes in the process parameters. The aim of the work is to determine the evolution (non-stationarity) of the yeast drying process. The mathematical model of the process (object) is used to determine the structure of the control system (controller type) and the settings of this controller. The basic process properties such as static characteristics, time constant and delay identified using recorded input and output signals or derived from physical laws. The direct approach does not focus on the exact approximation of the process.

During design control systems for processes in which the model parameters change their, it must be taken into account the stability of the control system. For such systems the robust control methodology is recommended [7, 8]. The robust control takes into account the model of object and is designed for correctly operates of the controller in uncertain object parameters conditions. The uncertainty of the model can be caused by: linearization of non-linear objects, inaccurate values of the model parameters, identification errors (disadvantages of the use of measurement data, too low sampling frequency, which impoverishes the characteristics of the object). In the robust control methodology the range of uncertain and the limits of properties variability are defined before mathematical modelling. The operation of robust control system adaptation within these limits and the change of the adopted process control principle is no necessary.

## 15.2 Food Raw Material Drying Process

Food raw material drying process produces cellular stress as presented in Fig. 15.1 [6]. The drying surface offsets into inside the organic material. The surface of the drying surface changes depends of shape of organic object (round grains, slices, agglomerations, a layer of wet powder or compound and complex shapes). The drying surface area effects the change in speed of moisture transport.

**Fig. 15.1** The offset of the drying surface during drying process of organic material [26]



In yeast drying case the temperature value and the rate of temperature change affects the fermentation capacity and lifespan [9, 19]. The level of fermentation capacity degradation depends on the dynamic of the drying process [13].

Different yeast strains used in industrial production distinguishes degrees of resistant to temperature [5, 24]. Moreover to immunize yeast for high temperature some additives like skim milk can be used [15].

The level of yeast degradation depends both on the drying method and on the parameters of the drying process (mainly temperature and its rate of change) [13]. When yeast is dried, the protoplasmic proteins are transformed from hydrosol to hydrogel. This leads to the reversible stop of the vital functions of the systems (anabiosis), depending on the amount of water left [14]. Adverse cellular stress occurs during drying [6]. For example, the optimal temperature of spouted bed is about 40 °C [20].

The drying process is the supply of warm air to the yeast. The yeast loses water during heating. This process is shown schematically in Fig. 15.2.

The drying process control is based on two values: yeast temperature  $T_Y$  and air temperature  $T_A$ . This is shown on the diagram in Fig. 15.3.

Industrial drying yeast process has non-stationary and non-linear character, therefore the control processes with classical control in this case system are difficult. Due to impossibility of using fixed parameters of the controller of the classical control system for the entire drying cycle, it is recommended to use complex control systems [20].

Process of organic object drying in dryer equipped with one heater located outside the drying chamber is presented in Fig. 15.4. In this schema the drying system

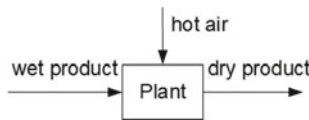


**Fig. 15.2** The yeast dehydration process

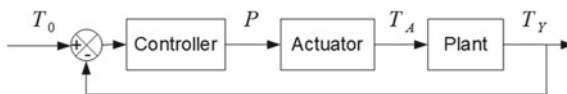


**Fig. 15.3** Control of yeast drying,  $T_0$ —setpoint signal,  $p$ —control signal,  $T_A$ —air temperature,  $T_Y$ —yeast temperature

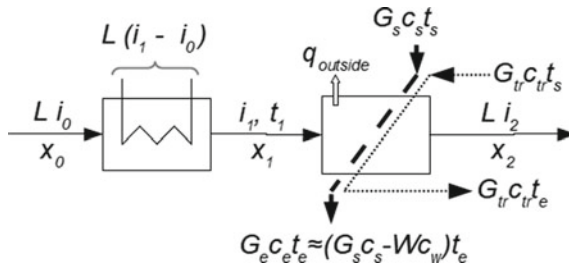
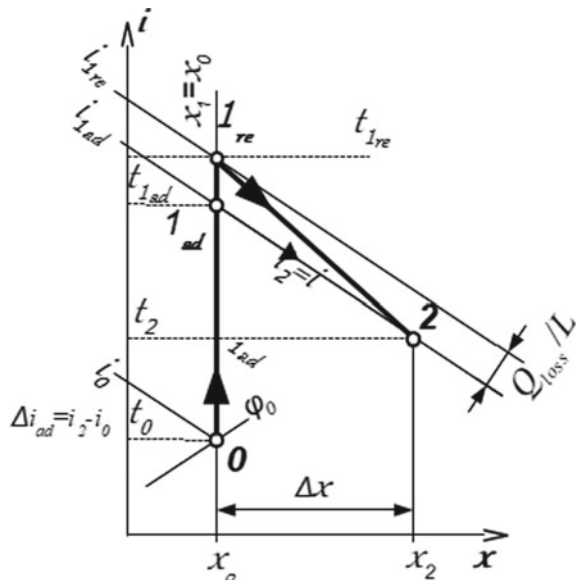


**Fig. 15.4** Block diagram of the continuous drying process (normal variant), (a), (b), (c) and (d)—heat streams flowing into the dryer, (e), (f), (g) and (h)—heat streams flowing out of the dryer; heat balance:  $a + b + c + d = e + f + g + h$ ; left block—preheater, right block—drying chamber.  $L$ —mass flow of dry air [kg/s],  $G$ —mass flow of moist material [kg/s],  $c$ —specific heat [kJ/(kg·K)],  $i$ —specific enthalpy [kJ/kg] of dry air,  $x$ —absolute humidity of air [kg of steam/kg of dry air],  $t$ —temperature [°C],  $W$ —mass flow of evaporated water from the material [kg/s]; indexes:  $s$ —initial value (start),  $w$ —water,  $e$ —finish value (end),  $tr$ —transporter, 0—atmospheric air, 1—heated air, 2—humidified air [26]

operates without air recirculation.

Figure 15.5 presents thermodynamic transformations accompanying drying process in the adiabatic process that is different than in the real case. In the schema the heat loss index  $Q_{loss}$  and the dry air mass flow  $L$  are localized. The difference between enthalpy of humid and atmospheric air is denoted by  $\Delta i_{ad}$  means.

**Fig. 15.5** Simplified enthalpy diagram with thermodynamic curves of the drying air in a dryer (normal variant), 0–1<sub>ad</sub>—heating in the adiabatic process, 0–1<sub>re</sub>—heating in the real process, 1<sub>ad</sub>–2—adiabatic dampening, 1<sub>re</sub>–2—real dampening.  $i$ —specific enthalpy [kJ/kg] of dry air,  $x$ —absolute humidity of air [kg of steam/kg of dry air],  $t$ —temperature [°C]  $\varphi_0$ —relative humidity of atmospheric air; indexes: 0—atmospheric air, 1—heated air, 2—humidified air,  $ad$ —adiabatic process (theoretic),  $re$ —real process (with losses) [26]



### 15.3 Subject of Research

The object of the research was the wet yeast layer dried by heated air flows. The air used for drying is mixed from two air streams: cool and heated air for obtaining right air temperature. The drying cycle takes more than seven hours and the yeast temperature cannot exceed  $50^{\circ}$ , which would destroy their functions.

The temperature of the yeast is monitored and controlled by air temperature according to the defined drying curve shown in Fig. 15.6. The temperature of the yeast layer is gradually raised during the drying cycle. The described process of the drying surface offsets in the wet organic layer with developed shape causes disruption in the drying control process. Examples of the series of drying cycles are shown in Fig. 15.6. Time series contains: setpoint signal, throttle opening, temperature under the sieve and temperature of the yeast layer. Disruption in the drying control process revealed in the increasing form the value of the error (the difference between the setpoint and wet layer temperature). Changing the sensitivity of the object caused by changes in the physical properties increases the risk of overheating the yeast. The current solution of this problem is step changing the controller's parameters during the process. The control system contains two sets of controller parameters. The controllers' parameters change is made at predefined time. Such a solution involves problems like: mismatching of to the moment of real change of the object's property and its dynamic. The change in properties can be gradual and complex while next parameters set for controller is introduced by step function.

Controlling of the organic product drying process with one PID controller proved to be ineffective. It was prepared a set of the controller parameters, used for a simple switching control model and adapted to changing object properties, as illustrated in

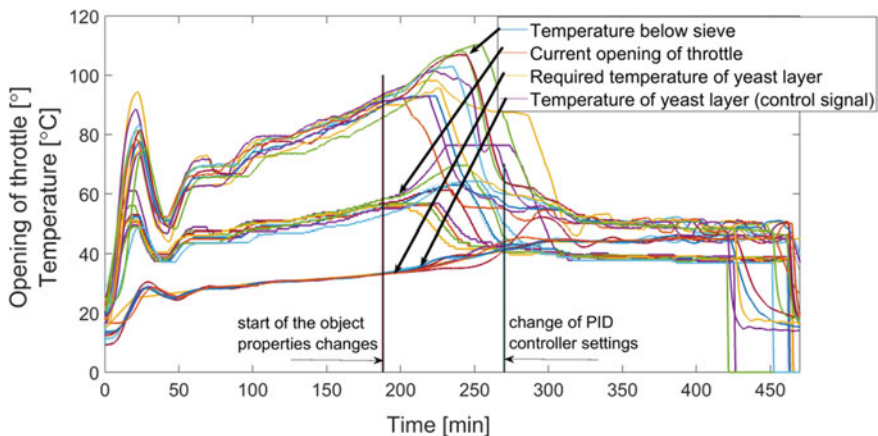


**Fig. 15.6** Example sets of signals recorded during drying process. Signals: setpoint trace—required temperature of yeast layer on sieve [ $^{\circ}\text{C}$ ], control signal—hot air throttle opening [ $^{\circ}\text{C}$ ], the controlled variables—temperature below sieve and yeast layer temperature [ $^{\circ}\text{C}$ ] [26]

the Fig. 15.6. The next settings are switched on according to the adopted model of the product temperature curve control.

## 15.4 Process Identification

There is a transport delay in the analyzed process, but it is difficult to determine because it requires carrying out an experiment that is currently not possible due to ongoing production. Process data is masked by previous states (large inertia of the process)—Fig. 15.7. The main transport delay is caused by the distance between the dried yeast and the heating element. It is possible to determine this delay analytically, but the knowledge of all geometric and technical parameters is needed (they are currently unavailable). At this stage of work, it is planned to identify the process without taking into account the delay. This delay is probably small compared to the inertia of the process (0.7 s—Fig. 15.8). The drying process begins in the 32.5 min of the cycle (beginning of the air temperature  $T_A$  increasing). The product's temperature value begins to grow from the 33.2 min recording of results ( $T_Y$ ). Thus, the transport delay is 0.7 min (42 s). Figure 15.8 shows the time courses of  $T_Y$  and  $T_A$  temperatures.

The recorded data comes from a closed system that includes an object, a measuring transducer, a controller and an actuator. Intuitively, it can be assumed that it is an inertial object with a delay, but it is uncertain. Yeast is an organic material in which various processes undergo. They have a significant influence on heat transfer. The

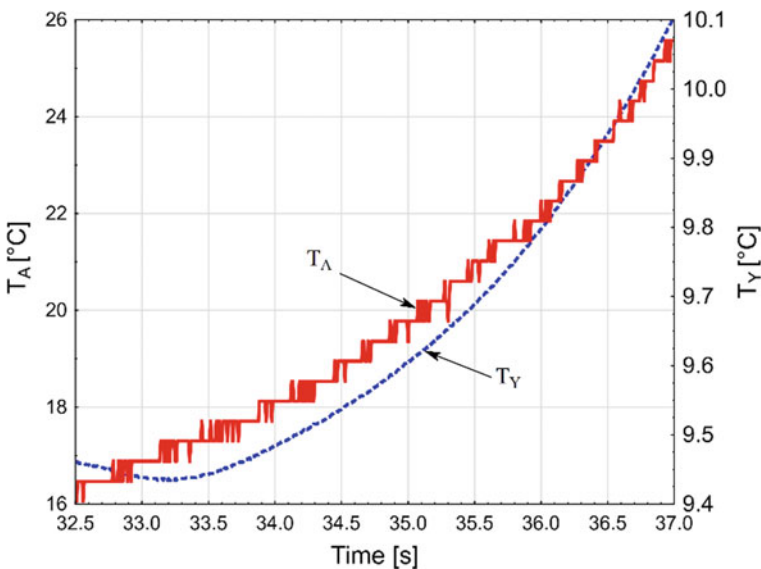


Fig. 15.7  $T_A$  and  $T_Y$  temperature in at the beginning of the process

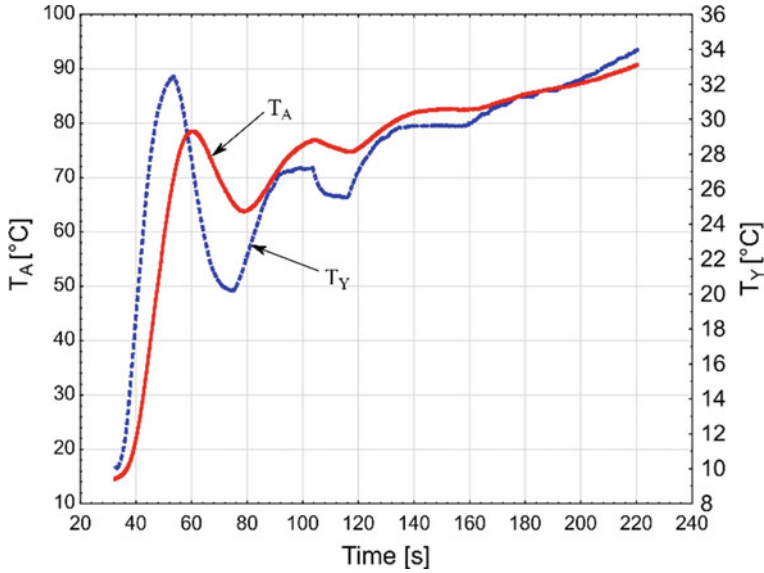


Fig. 15.8  $T_A$  and  $T_Y$  temperature in analyzed process

parameters of the object are changing, so the object is nonstationary. The recorded results come from a closed, stable system. Models (discrete operator transmissions) for different time intervals were determined in order to examine whether the system is non-stationary.

**Identification of model parameters describing the relationship between air temperature and product temperature.**

The model describing the relationship between the discrete value of air temperature and product temperature can be described by a discrete equation (with aggregated parameters) of the form:

$$T_y(k) + a_1 T_y(k - 1) - \dots - a_n T_y(k - n) = b_0 T_A(k - h) + b_1 T_A(k - 1 - h) + \dots + b_n T_A(k - n - h) \quad (15.1)$$

where  $h$  is a discrete time delay,  $a_i, b_i$  are model parameters.

The product temperature values  $T_y(k)$  can be determined from the model as follows:

$$\hat{T}_y(k) = b_0 T_A(k - h) + \dots + b_n T_A(k - n - h) - a_1 T_y(k - 1) - \dots - a_n T_y(k - n) \quad (15.2)$$

Using the reverse operator and substituting:

$$\nabla T_y = T_y(k) - T_y(k - 1) = (1 - z^{-1})T_y \quad (15.3)$$

$$\nabla T_A = T_A(k) - T_A(k-1) = (1 - z^{-1})T_A \quad (15.4)$$

$$A^*(z) = a_1z^{-1} - a_2z^{-2} - \dots - a_nz^{-n} \quad (15.5)$$

$$B(z) = (b_0 + b_1z^{-1} + b_2z^{-2} + \dots + b_nz^{-n})z^{-h} \quad (15.6)$$

we obtain

$$\hat{T}_y(k) = B(z)T_A(k) + A^*(z)T_y(k) \quad (15.7)$$

The above model has been supplemented by external disturbances:

$$\hat{T}_y(k) = B(z)T_A(k) + A^*(z)T_y(k) + \eta(k) \quad (15.8)$$

Using the transformation

$$T_y(k) - A^*(z)T_y(k) = B(z)T_A(k) + \eta(k) \quad (15.9)$$

$$A(z) = 1 - A^*(z) \quad (15.10)$$

leads to

$$T_y(k) = \frac{B(z)}{A(z)}T_A(k) + \frac{1}{A(z)}\eta(k) \quad (15.11)$$

The first part of the equation describes the process of heat exchange between the air temperature  $T_x(k)$  and the mass of product  $T_y(k)$ . The second part of the equation takes into account interference effects in this model. The dependency corresponding to the part of the first equation can be written in the form of a discrete transfer function as (with a transport delay):

$$G(z) = \frac{T_y(z)}{T_A(z)} = \frac{B(z)}{A(z)} = \frac{b_0z^{-1} + b_1z^{-2} + b_2z^{-3}}{1 + a_1z^{-1} + a_2z^{-2} + a_3z^{-3}}z^{-h} \quad (15.12)$$

where  $z^{-1}$  is the backward difference operator shift ( $i = 1, 2, 3, \dots, n$ ) and  $h$  is the transport delay.

Finally, the heat exchange process is described by third order discrete transmission without delay  $h$  as

$$G(z) = \frac{b_0z^{-1} + b_1z^{-2} + b_2z^{-3}}{1 + a_1z^{-1} + a_2z^{-2} + a_3z^{-3}} \quad (15.13)$$

Parameters of identified model are presented in Table 15.1.



**Table 15.1** Parameters of identified model

Interval no.	Sample no.	b <sub>0</sub>	b <sub>1</sub>	b <sub>2</sub>	a <sub>1</sub>	a <sub>2</sub>	a <sub>3</sub>
1	0–5000	0.0451	–0.0067	–0.0379	0.3713	0.3191	0.3085
2	3000–8000	0.0595	–0.0153	–0.0437	0.3380	0.3309	0.3300
3	5000–10000	0.0447	–0.0093	–0.0349	0.3523	0.3195	0.3272
4	10000–15000	0.0104	0.0019	–0.0121	0.3466	0.3348	0.3183
5	15000–20000	0.0246	0.0040	–0.0284	0.3269	0.3212	0.3515
6	17500–22500	0.0062	0.0216	–0.0276	0.3355	0.3199	0.3441

**Table 15.2** The roots of discrete transmittances

Sample no.	Re1	Im1	Re2	Im2	Re3	Im3
0–5000	–0.3141	0.4583	–0.3141	–0.4583	0.9994	0
5000–10000	–0.3236	0.4718	–0.3236	–0.4718	0.9995	0
10000–15000	–0.3266	0.4601	–0.3266	–0.4601	0.9998	0
15000–20000	–0.3365	0.4882	–0.3365	–0.4882	0.9998	0

The model parameters change with the drying time. The roots of discrete transmittances of the closed system are determined in Table 15.2. The roots (zeros of the characteristic equation) were calculated for the time periods for which discrete transmittances were determined—Table 15.2.

The system is stable if and only if

$$\bigwedge_{i \in 1, k} |z_i| < 1 \tag{15.14}$$

where  $z_i$  are the roots of the control system with closed loop (feedback) and  $k$  is the number of roots.

Root No. 3 (Re3) is located very close to the unit circle. It means that the system is very close to the stability limit.

The identification concerns separated elements of the system like actuator and object as well as object including a dryer and product. The actuator element that was the throttle can be characterized by the linear transfer function, whereas, the object can be characterized by the non-linear function.

Nonlinear ARX (AutoRegressive with eXogenous inputs) models have structure:

$$y(t) = f(y(t - 1), \dots, y(t - n_a), u(t - n_k), \dots, u(t - n_k - n_b + 1)) \tag{15.15}$$

where  $u$  and  $y$  are finite numbers of previous inputs and outputs,  $n_a$  and  $n_b$  are numbers of past output and input terms, which are used to predict the output and  $n_k$  is the delay from the input to the output, defined as the number of samples.

In Fig. 15.9 an examples of measured process signals and simulated model outputs

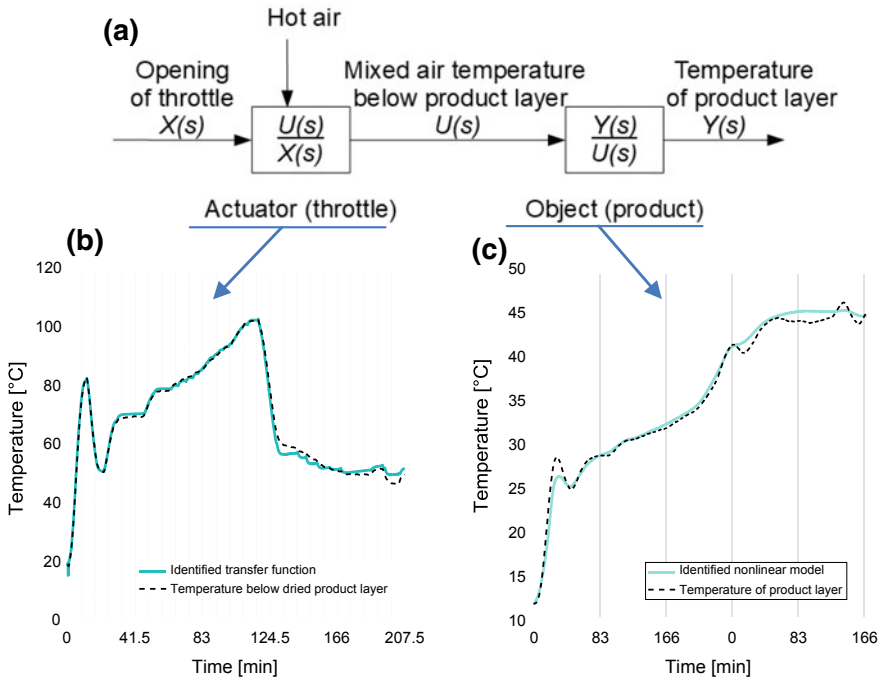


**Fig. 15.9** Examples of measured process signals and simulated model output **a** schema of the actuator and object inputs and outputs, **b** actuator output signal (temperature below dried product layer), **c** object output signal (temperature of product)

are presented. The model of actuator was identified by linear transfer function (15.16). Fit to estimation data performs 92.25% ( $FPE^1 = 1.957$ ,  $MSE^2 = 1.956$ ).

$$\frac{U(s)}{X(s)} = \frac{-650.4 \cdot s^4 - 199.2 \cdot s^3 + 5 \cdot s^2 + 0.08 \cdot s + 3.2e - 6}{s^5 + 1026 \cdot s^4 + 360.1 \cdot s^3 + 6.8 \cdot s^2 + 0.03 \cdot s + 2e - 6} \quad (15.16)$$

The model of object was estimated by nonlinear ARX model using elements (15.17). Estimation fit to data perform 99.85% ( $FPE = 0.000159$ ,  $MSE = 0.000155$ )

$$y1(t - 1), y1(t - 2), u1(t - 1), u1(t - 2) \quad (15.17)$$

Final prediction error (FPE): 0.0001701, Loss function: 0.0001698. Fit to working data: 93.32%

<sup>1</sup>FPE: Final prediction error means percent fit to estimation data.

<sup>2</sup>MSE: Mean-square error.

## 15.5 Process Simulation

The first stage of the control developing was registration of the signals from the real object. Second stage was identification of the object and estimation of mathematical model of the object. The identification concerns separated elements of the system like actuator and object as well as object including a dryer and product. Similarly, for the estimation there were exposed the complete time series (symbol AB) of the process and parts (symbols A and B) as results of division in the moment of change of controller's set parameters. The third stage was the preparation of the systems for simulation using the classical PID controlled. For ten drying cycle the set of transform functions has been prepared. The functions have different order value of transform functions (characteristic equation). During the identification of the mathematical models, the order of characteristic equation of the objects and function coefficients are adapted. Additionally, the estimation of nonlinear function to identify the model of the object was conducted.

Identification of the mathematical model was conducted separately for the first (A) and second (B) parts of drying cycle. Recorded signals were also used to identify process elements mentioned in Fig. 15.3. Due to the use of a temperature below the sieve signal, it was possible to identify the properties of the yeast layer and process analysis.

For improvement of the currently operating control system the mathematical model was used to optimize the PID controllers' parameters and for optimize moment of switching the PID controller settings. In the Fig. 15.6 can be seen fluctuations in the input and control signals occurs before the switching of the PID controller settings. The control system simulation with identified objects allowed for correction of the time of the controller's settings. The system simulation results after correction of the changeover time of the controller's settings presents Fig. 15.10. The object is

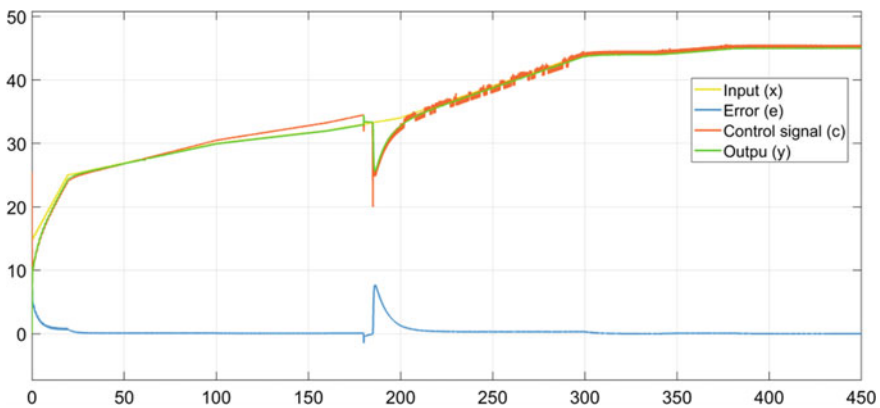


**Fig. 15.10** Simulation of drying process characterized by two transfer function  $G_A$ ,  $G_B$ , and two controllers PI ( $K_p = 1.7$ ,  $K_i = 0.785$ ) and PID ( $K_p = 1.3$ ,  $K_i = 0.312$ ,  $K_d = 0.758$ ), with limited output in range from 20 to 80 [°C] switched in 180th time unit of simulation [26]

identified by two transfer function  $G_A$  and  $G_B$ . The switch time is set in 180th time unit of simulation. The simulation results are presented in Fig. 15.10. Such control system should protect the product from overheating.

$$G_B = \frac{34s^3 + 2.5s^2}{s^4 + 33.4s^3 + 2.5s^2} \quad (15.18)$$

$$G_B = \frac{25s^3}{s^4 + 25.1s^3} \quad (15.19)$$

### 15.5.1 Robust Uncertainty Principles Application

In order to protect drying product from overheating, the robust method was used. Firstly, signals recorded from the real process were used to identify elements. Secondly, the mathematical model of the object was prepared and applied for the robustness controller. For the characteristic equation coefficients the uncertainty in the range of  $\pm 20\%$  of nominal values was determined. In the Fig. 15.11 a set of the step responses is presented. The set contains response of PI control systems in the first part (A) of the drying cycle, PID controller in the second part (B) of the drying cycle and the robust controller controlling the process in whole cycle. In this case the object transmittance was identified for signals recorded in both parts of the process (parts A and B).

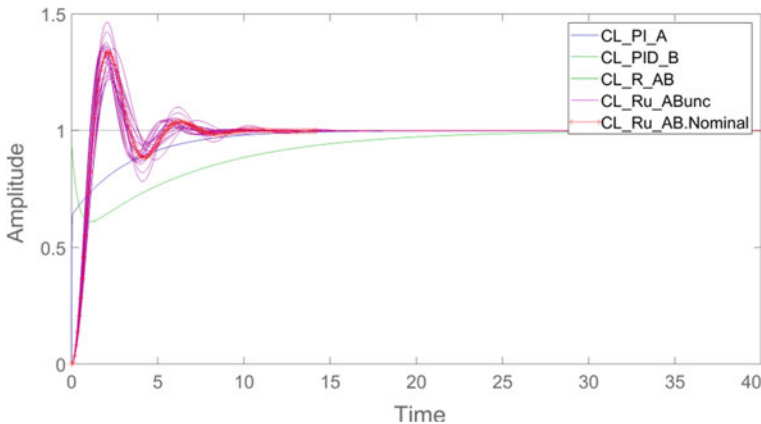


**Fig. 15.11** Step response for mathematical models of feedback systems consists of controllers and transfer function of objects: CL\_PI\_A—PI controller and transfer function of part A, CL\_PID\_B—PID controller and transfer function of part B, CL\_R\_AB—Robust controller and transfer function of parts A+B [26]

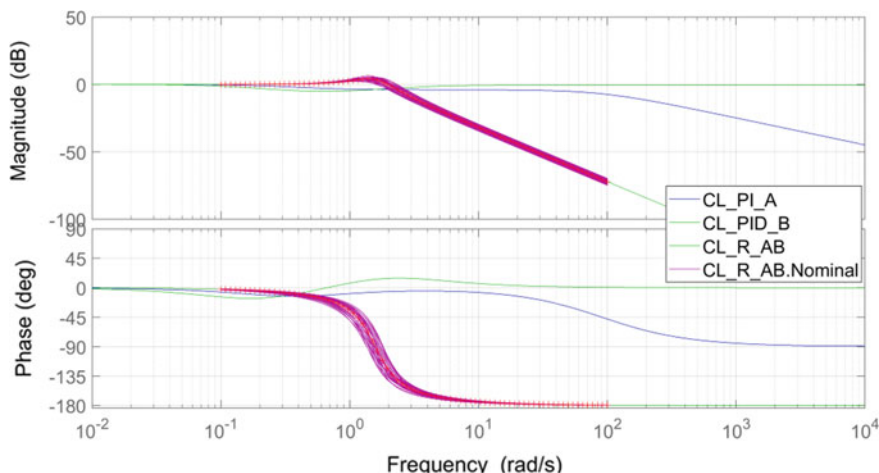


**Fig. 15.12** Sensitivity analysis **a** Bode plots for closed-loop systems and **b** Nyquist plot for mathematical models of open-loop systems consists of controllers and transfer function of objects: PI\*G<sub>A</sub>—PI controller and transfer function of part A, PID\*G<sub>B</sub>—PID controller and transfer function of part B, C<sub>R</sub>\*G<sub>AB</sub>—Robust controller and transfer function of parts A+B [26]

Simulation with the robustness controller allows controlling the process quality in whole cycle, whilst using of the PI controller during second part (B) and PID controller in the first part (A) causes instability of system in both cases.

Using the inverted model (15.18), the sensitivity of the system was simulated and results are presented in Fig. 15.12.

$$G_S = 1/G_{model} \tag{15.20}$$

Figure 15.11 illustrates the dynamic characteristics of control systems with PI, PID and robustness controllers. The use of a robustness regulator eliminates variation of the product temperature caused by a sudden change of the object’s properties.

## 15.6 Conclusion

Drying of organic products can have a non-linear character caused by the technology used and the change of the physical properties of the object. Changing the physical properties of the object causes an increase in the temperature error value of the object relative to the planned drying curve. This character of the transformation increases the risk of overheating the yeast.

The yeast drying is a non-stationary process, confirmed by changes in transmittance coefficients. Analyzing the position of the poles of the system, it can be state that the reserve of stability is very small and decreases over time. It means that

changes in the properties of the object can lead to the loss of stability of the system (process) that is confirmed by industrial results. Change of the object's properties forces change of the controller's settings during the process. The robust control is known in the literature, but rarely used in practice for non-linear process control. The knowledge about the object's properties will enable selection of the appropriate structure of the control system.

## References

1. G. Battistelli, D. Mari, D. Selvi, P. Tesi, Direct control design via controller unfalsification. *Int. J. Robust Nonlinear Control* **28**(12), 3694–3712 (2017)
2. D. Bayrock, W.M. Ingledew, Mechanism of viability loss during fluidized bed drying of baker's yeast. *Food Res. Int.* **30**(6), 417–425 (1997). [https://doi.org/10.1016/S0963-9969\(97\)00072-0](https://doi.org/10.1016/S0963-9969(97)00072-0)
3. T. Borowy, Everything about yeast (in Polish). *Mistrz branży* (2014). <http://mistrzbranzy.pl/artykuly/pokaz/Wszystko-o-drozdach-1721.html>
4. R. Cechowicz, P. Staczek, Computer supervision of the group of compressors connected in parallel. *Maint. Reliab.* **16**(2), 198–202 (2014)
5. K. Charoensoparat, P. Thanonkeo, S. Thanonkeo, M. Yamada, Ethanol production from Jerusalem artichoke tubers at high temperature by newly isolated thermotolerant inulin-utilizing yeast *Kluyveromyces marxianus* using consolidated bioprocessing. *Antonie Leeuwenhoek* **108**(1), 173–190 (2015). <https://doi.org/10.1007/s10482-015-0476-5>
6. E. Gamero-Sandemtrio, L. Payá-Tormo, R. Gómez-Pastor, A. Aranda, E. Matallana, Non-canonical regulation of glutathione and trehalose biosynthesis characterizes non-*Saccharomyces* wine yeasts with poor performance in active dry yeast production. *Microb. Cell* **5**(4), 184–197 (2018)
7. C.E. Garcia, M. Morari, Internal model control. A unifying review and some new results. *Ind. Eng. Chem. Process. Des. Dev.* **21**, 308–323 (1982)
8. C.E. Garcia, M. Morari, Internal model control. 2. Design procedure for multivariable systems. *Ind. Eng. Chem. Process. Des. Dev.* **24**, 472–484 (1985)
9. P. Gervais, I. Maranon, Effect of the kinetics of temperature variation on *Saccharomyces cerevisiae* viability and permeability. *Biochem. Biophys. Acta* **1235**(1), 52–56 (1995)
10. P. Harris, M. Arafa, G. Litak, C.R. Bowen, J. Iwaniec, Output response identification in a multistable system for piezoelectric energy harvesting. *Eur. Phys. J. B* **90**(1), 1–11 (2017)
11. H. Hjalmarsson, From experiment design to closed-loop control. *Automatica* **41**, 393–438 (2005)
12. D.M. Jenkins, C.D. Powell, T. Fischborn, K.A. Smart, Rehydration of active dry brewing yeast and its effect on cell viability. *J. Inst. Brew.* **117**(3), 377–382 (2011)
13. A. Kamińska-Dwórznička, A. Skoniecka, The influence of drying methods, parameters and the way of storage on the activity of bakery yeasts (in Polish). *Zeszyty Problemowe Postępów Nauk Rolniczych* **573**, 35–42 (2013)
14. T. Kudra, C. Strumiłło, *Thermal processing of biomaterials*. Gordon and Breach Science. OPA Amsterdam (1998)
15. S.B. Lee, W.S. Choi, H.J. Jo, S.H. Yeo, H.D. Park, Optimization of air-blast drying process for manufacturing *Saccharomyces cerevisiae* and non-*Saccharomyces* yeast as industrial wine starters. *AMB Express* **6**(1), 105 (2016)
16. G. Litak, R. Rusinek, Identification of turning and milling processes by stochastic Langevin equations, in *4th IEEE International Conference on Nonlinear Science and Complexity* (2012), pp. 41–44
17. L. Ljung, *System identification: theory for the user*, 2nd edn. (Prentice Hall PTR, Upper Saddle River, 1999). <http://dx.doi.org/10.1002/047134608x.w1046>

18. A. Martynenko, Computer vision for real-time control in drying. *Food Eng. Rev.* **9**(2), 91–111 (2017). <https://doi.org/10.1007/s12393-017-9159-5>
19. F.I. Mensonides, S. Brul, K.J. Hellingwerf, B.M. Bakker, M.J. Teixeira de Mattos, A kinetic model of catabolic adaptation and protein reprofiling in *Saccharomyces cerevisiae* during temperature shifts. *FEBS J.* **281**(3), 825–841 (2014)
20. D. Muhammad, Z. Ahmad, N. Aziz, Implementation of internal model control (IMC) in continuous distillation column, in *Proceedings of the 5th International Symposium on Design, Operation and Control of Chemical Processes* (2010), pp. 812–821
21. M. Paślawska, Influence of the fountain drying temperature on the dewatering kinetics and yeast viability (in Polish). *Inżynieria Rolnicza* **5**(103), 161–166 (2008)
22. W. Samociuk, Z. Krzysiak, M. Szmigielski, J. Zarajczyk, Z. Stropek, K. Gołacki, G. Bartnik, A. Skic, A. Nieoczym, Modernization of the control system to reduce a risk of severe accidents during non-pressurized ammonia storage (in Polish). *Przemysł Chemiczny* **95**(5), 1000–1003 (2016). <https://doi.org/10.15199/62.2016.5.29>
23. W. Samociuk, A. Wyciszkiewicz, K. Gołacki, T. Otto, Risk of catastrophic failure of the reactor for urea synthesis (in Polish). *Przemysł Chemiczny* **96**(8), 1763–1766 (2017). <https://doi.org/10.15199/62.2017.8.32>
24. A. Techaparin, P. Thanonkeo, P. Klanrit, High-temperature ethanol production using thermotolerant yeast newly isolated from Greater Mekong Subregion. *Braz. J. Microbiol.* **48**(3), 461–475 (2017)
25. P. Wolszczak, K. Łygas, G. Litak, Dynamics identification of a piezoelectric vibrational energy harvester by image analysis with a high speed camera. *Mech. Syst. Signal Process.* **107**, 43–52 (2018)
26. P. Wolszczak, W. Samociuk, The control system of the yeast drying process, in *MATEC Web of Conferences*, vol. 241 (2018), p. 01022. <https://doi.org/10.1051/mateconf/201824101022>
27. L.-P. Yang, S.-L. Ding, G. Litak, E.-Z. Song, X.-Z. Ma, Identification and quantification analysis of nonlinear dynamics properties of combustion instability in a diesel engine. *Chaos* **25**, 013105-1–013105-13 (2015)